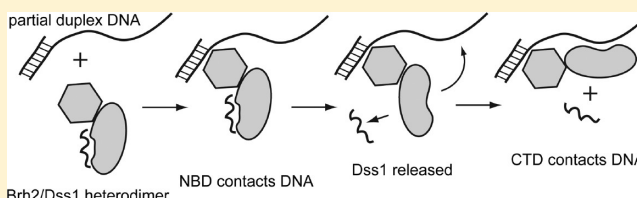


Dss1 Release Activates DNA Binding Potential in Brh2

Qingwen Zhou, Milorad Kojic, and William K. Holloman*

Department of Microbiology and Immunology and Weill Cornell Cancer Center, Weill Cornell Medical College, New York, New York 10065, United States

ABSTRACT: Dss1 is an intrinsically unstructured polypeptide that partners with the much larger Brh2 protein, the BRCA2 ortholog in *Ustilago maydis*, to form a tight complex. Mutants lacking Dss1 have essentially the same phenotype as mutants defective in Brh2, implying that through physical interaction Dss1 serves as a positive activator of Brh2. Dss1 associates with Brh2 through an interaction surface in the carboxy-terminal region. Certain derivatives of Brh2 lacking this interaction surface remain highly competent in DNA repair as long as a DNA-binding domain is present. However, the Dss1-independent activity raises the question of what function might be met in the native protein by having Brh2 under Dss1 control. Using a set of Brh2 fusions and truncated derivatives, we show here that Dss1 is capable of exerting control when there is a cognate Dss1-interacting surface present. We find that association of Dss1 attenuates the DNA binding potential of Brh2 and that the amino-terminal domain of Brh2 helps evict Dss1 from its carboxy-terminal interaction surface. The findings presented here add to the notion that Dss1 serves in a regulatory capacity to dictate order in association of Brh2's amino-terminal and carboxy-terminal domains with DNA.



Repair of DNA containing single-stranded regions, double-strand breaks, or gaps by homologous recombination requires Rad51 in eukaryotes. Rad51 assembles into a complex with single-stranded DNA (ssDNA) to form a nucleoprotein filament, which is the catalytically active form of Rad51 for promoting homologous pairing and DNA strand exchange.^{1–4} Important regulators of Rad51 strand exchange activity are the mediators, factors that allow Rad51 access to ssDNA coated with the heterotrimeric single-strand binding protein replication protein A (RPA). Widespread throughout the eukaryotic domain are mediators of the BRCA2 class, the founding member being a human breast cancer tumor suppressor.⁴ BRCA2 homologues in different taxonomic groups are divergent in size and sequence, but two defining features prevail. These are the BRC repeats, a motif often found reiterated that interacts with Rad51,^{5,6} and the Dss1/DNA-binding domain (DBD) in the C-terminal region, which is composed of a helix-rich region and a tandem array of oligonucleotide/oligosaccharide binding (OB) fold modules with the potential for binding ssDNA.⁷ Both the number of BRC repeats and the number of OB folds vary depending on the organism.⁸ The most highly conserved region among the BRCA2 family members is the helix-rich domain and adjacent OB1 fold of the C-terminal region. This portion of the protein is bound tightly by a small intrinsically unstructured polypeptide, DSS1, which acts as a regulator of BRCA2.⁹ By sequence alignment, the residues forming the DSS1-interacting interface comprise the most highly conserved region within the BRCA2 family of proteins.

Brh2 is the BRCA2 ortholog in the fungus *Ustilago maydis*.¹⁰ It could be considered a streamlined version of the much larger mammalian protein, at one-third the size and having only a

single BRC motif and a carboxy-terminal domain (CTD) with two rather than three OB folds as in the mammalian DBD. As with the mammalian protein, a coiled coil or tower emerges from the second OB fold, and another Rad51-interacting region (CRE) unrelated to the BRC is present at the extreme C-terminus.¹¹ From sequence alignment and comparison with the crystal structure of the mammalian protein, it is apparent that almost all of the DSS1-contacting residues in the BRCA2 DBD are identical or conservatively substituted in Brh2. Likewise, the BRCA2-contacting residues of DSS1 are conserved in the ortholog (Dss1) from *U. maydis*, and the protein forms a tight heterodimeric complex with Brh2.^{9,12} The interaction interface appears to be very important for biological activity as mutation of a single Dss1-contacting residue results in a loss of function.¹¹ Mutants lacking Brh2 are extremely sensitive to DNA damage, are deficient in recombination, exhibit chromosome rearrangements, and are defective in meiosis.¹⁰ Similarly, deletion of the gene encoding Dss1 results in essentially the same phenotype as the brh2 mutant, implying that Dss1 serves as a positive activator of Brh2,⁹ yet by expressing a Brh2 mutant variant without its carboxy-terminal region encompassing the entire CTD or else replacing the CTD with a heterologous DNA-binding domain from the RPA 70 kDa subunit with no ability to interact with Dss1, one could reverse the mutant phenotype and substantially restore the biological function even in the absence of Dss1.¹³ These results suggested that Dss1 exerts a negative regulatory effect on Brh2 because in the absence of the Dss1-interacting region DNA

Received: August 17, 2012

Revised: October 24, 2012

Published: October 24, 2012

repair activity was restored. Subsequently, it was found that the amino-terminal portion of Brh2 (Brh2^{NT}) contained a separate DNA-binding domain (NBD) distal to the BRC motif that appeared to be partially redundant with the C-terminal CTD, accounting for the biological activity of the N-terminal fragment of Brh2.¹⁴

A challenge in understanding the mechanism of Brh2 action has been to explain the seemingly positive and negative aspects of Dss1 regulation, i.e., that Dss1 appears to be necessary for DNA repair activity in the context of full-length Brh2 protein but seems to be dispensable when its cognate interaction site in the Brh2 CTD is removed. A clue about the role of Dss1 in controlling Brh2 was revealed through studies of the DNA binding kinetics of Brh2.¹⁵ When the Brh2–Dss1 heterodimer was tested for binding activity, the rate of formation of protein–DNA complexes was slow by comparison with the fast binding exhibited by Brh2^{NT}, the Dss1-independent Brh2 N-terminal fragment. Because DNA binding reactions are generally thought to be diffusion-controlled and thus are fast, the kinetics exhibited by the Brh2–Dss1 complex seemed anomalous. This led us to consider the possibility that some step other than diffusion was rate-limiting in the binding of the Brh2–Dss1 protein to DNA. Indeed, we observed that Dss1 was no longer associated with Brh2 in the DNA-bound form, raising the possibility that ejection of Dss1 from Brh2 might result in a change in state to allow DNA binding or stabilization of the DNA-bound Brh2 complex. Thus, it seemed that some conformational change in Brh2 involving a dynamic association with Dss1 might underpin the DNA binding kinetics.

Here we have examined the dissociation of Dss1 from Brh2 to gain insight into a possible role in regulating DNA binding. To implement the study, we used a series of Brh2 derivatives with truncations or substitutions of the DNA-binding domains.

■ EXPERIMENTAL PROCEDURES

***U. maydis* Methodology.** Manipulations of *U. maydis* strains, culture methods, gene transfer procedures, and survival after UV irradiation have been described previously (see refs 16 and 17 and references cited therein). The following strains were utilized: UCM350 (nominal wild type), UCM565 (*brh2*), and UCM637 (*brh2 dss1*). Genes encoding Brh2 and its derivatives, including truncations and synthetic variants with heterologous DNA-binding domain insertions, were expressed in *U. maydis* under the *gap* (glyceraldehyde-3-phosphate dehydrogenase) promoter in self-replicating plasmids.

DNA Substrates. The DNA oligonucleotides (Eurofins MWG/Operon) used as substrates were 60-mers based on nucleotides 103–162 from bacteriophage ϕ X174 sequence or an 80-mer based on nucleotides 22–101 from plasmid pBluescript II SK+ (Stratagene). The oligonucleotides contained 5'-IRD800 or 3'-biotin modifications as indicated. All DNA concentrations are given in terms of moles of oligonucleotide.

DNA Binding Assays. Reaction mixtures (15 μ L) containing 25 mM HEPES buffer (pH 7.5), 40 mM KCl, 1 mM dithiothreitol, 3.3 nM IRD800 oligonucleotide, and protein as indicated were incubated, unless otherwise indicated, at 32 °C for up to 40 min. Glutaraldehyde was added to a final concentration of 0.02%, and 10 min later, the reaction was quenched by addition of 0.1 M Tris-HCl (pH 8.0). Reaction mixtures were electrophoresed in 1% agarose gels and analyzed for DNA–protein complexes using a LI-COR Odyssey infrared imaging platform.

Affinity Bead Pull-Down Procedures. Reactions (30–50 μ L) were performed in 35 mM MOPS buffer (pH 7.5), 40 mM KCl, 1 mM dithiothreitol, 0.001% NP-40, 60-mer oligonucleotide, and protein as indicated. To capture biotinylated oligomers, one-sixth volume of a suspension of streptavidin-coated MagneSphere paramagnetic particles (Promega) was added. For MBP–Brh2 and derivatives, one-sixth volume of amylose resin (New England Biolabs) slurry was added. For His–Dss1 and associated Brh2 complexes, one-sixth volume of Ni²⁺-charged nitrilotriacetate agarose (NTA) bead (Novagen) slurry was added. After being continuously gently mixed for 10 min, particles or beads were separated (magnetic field or centrifugation), and bound and unbound components were analyzed by sodium dodecyl sulfate (SDS) gel electrophoresis. Brh2 was detected by protein staining (Simply Blue Safe stain, Life Technologies). DNA was tracked when required by addition of 5'-IRD800 oligonucleotide. His–Dss1 was detected after Western blot transfer to a nitrocellulose membrane using an anti-six-His monoclonal antibody (Sigma-Aldrich) and a goat anti-mouse IRD680 secondary antibodies (LI-COR Biosciences). Visualization and quantification were conducted using the LI-COR Odyssey platform and ImageQuant TL software (GE Healthcare).

Protein Preparation and Methods. Brh2 and Brh2^{CT} (Brh2 Δ N505) were purified as maltose binding protein (MBP) fusions in complex with hexahistidine (His)-tagged Dss1 or free of His–Dss1, as described previously as was Brh2^{NT} (Brh2 Δ C551), and His–Dss1.^{11,14,15,18} The construction of Brh2 Δ C362::OB-AB, Brh2 Δ 362–493, and Brh2 Δ 362–493::OB-AB was detailed previously.¹⁹ The latter two variants were purified as MBP fusions in complexes with His–Dss1 for biochemical analysis after overexpression in *Escherichia coli* along the lines described for the MBP–Brh2–His–Dss1 complex. Briefly, purification involved sequential affinity chromatography on Ni²⁺-NTA agarose, amylose resin, monoQ beads, and HiTrap heparin-agarose (GE Healthcare).

■ RESULTS

Requirement for Dss1 in Brh2-Promoted DNA Repair Function. It was shown previously that the two different DNA-binding domains of Brh2, namely, the NBD located in the N-terminal region and the Dss1-interacting OB fold-containing CTD, both contribute to maintaining appropriately regulated Brh2 functional activity.¹⁹ However, a remarkable degree of architectural plasticity was noted in domain structure utilization in response to DNA damage or replication fork stalling. In particular, the domain requirement for activity in promoting repair after DNA damage was found to be flexible. The NBD or CTD could be either eliminated or replaced by a heterologous DNA-binding domain with little loss in the ability to support survival after UV irradiation. In instances in which the NBD was eliminated or replaced by a heterologous DNA-binding domain but the CTD was retained, we were curious about the disposition of Dss1. Would it still be necessary for Brh2 functional activity, and would the loss be concomitant with DNA binding?

We tested a set of Brh2 truncations and synthetic fusions for DNA repair activity regulated by Dss1 as measured *in vivo*. This was performed by expressing individual Brh2 constructs in either the *brh2* single mutant or *brh2 dss1* double mutant and then measuring the extent that the truncations or fusions were able to complement the mutant phenotype and promote survival after UV irradiation (Figure 1). It was noted that Brh2

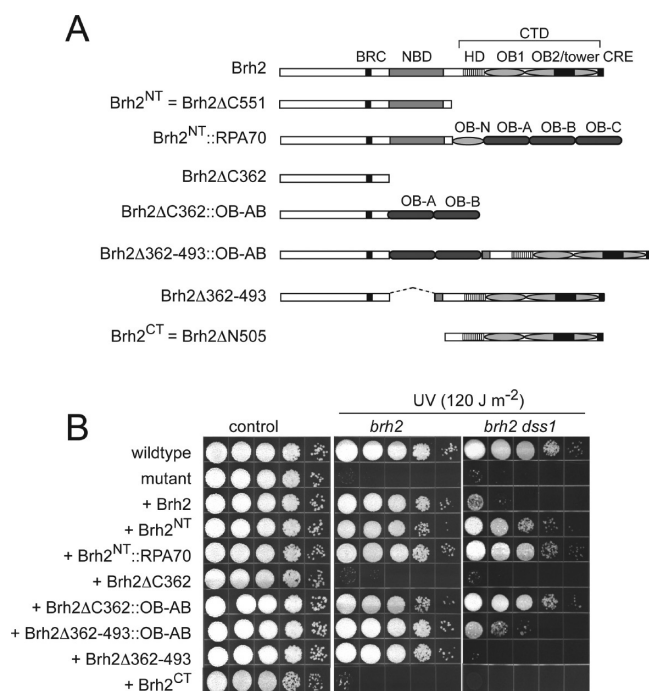


Figure 1. Dss1 dependence of Brh2 derivatives. (A) Schematic illustration of the domain maps of Brh2 and derivative variants. Approximate locations of the BRC and CRE Rad51-interacting regions (black bars), the N-terminal DNA-binding domain or NBD (gray bar), and the C-terminal domain or CTD that includes the helix-rich domain (HD) and two tandem OB modules (ovals), the second of which has a coiled coil tower region, are shown. OB folds (N, A, B, and C) from the RPA70 subunit that are present in Brh2 derivatives (rounded dark gray rectangles). (B) Survival of *brh2* and *brh2 dss1* mutant strains expressing the indicated Brh2 derivative after UV irradiation. Cell suspensions were adjusted to a density of $\sim 2 \times 10^7$ cells/mL and diluted in 10-fold serial dilutions, and aliquots (10 mL) were spotted from left to right. Survival is apparent as the growth of colonies 3 days post-irradiation.

variants lacking the CTD but still capable of promoting survival were active in a manner that was independent of Dss1. This class of variants included the synthetic construct Brh2ΔC362::OB-AB composed of a Brh2 N-terminal fragment containing the BRC motif fused to a heterologous DNA-binding domain consisting of the OB-A and OB-B folds (OB-AB) of the 70 kDa subunit of the single-stranded DNA binding protein RPA. In contrast, Brh2 derivatives retaining the native CTD were all dependent on Dss1, including Brh2Δ362–493::OB-AB, a derivative of the synthetic construct described above (Brh2ΔC362::OB-AB) with the CTD fused to the carboxy terminus. The presence of the short basic KRPR tract (residues 496–499 lying between the NBD and HD depicted in the figure), which fits the loose [K(K/R)X(K/R)] consensus of monopartite nuclear localization signals,²⁰ raised concern that poor activity conferred by some of the constructs might stem from a defect in nuclear localization. However, in previous work, we noted that deletion of this sequence or mutation of all four residues to alanine had no discernible effect on the functional activity of Brh2,¹⁶ suggesting that nuclear transport of Brh2 does not require the nuclear import system or that some other yet unrecognized nonconsensus sequence might serve in this capacity. This caution aside, it appears that coupling the native CTD to an active Brh2 fragment or synthetic fusion brings the entity under the control of Dss1.

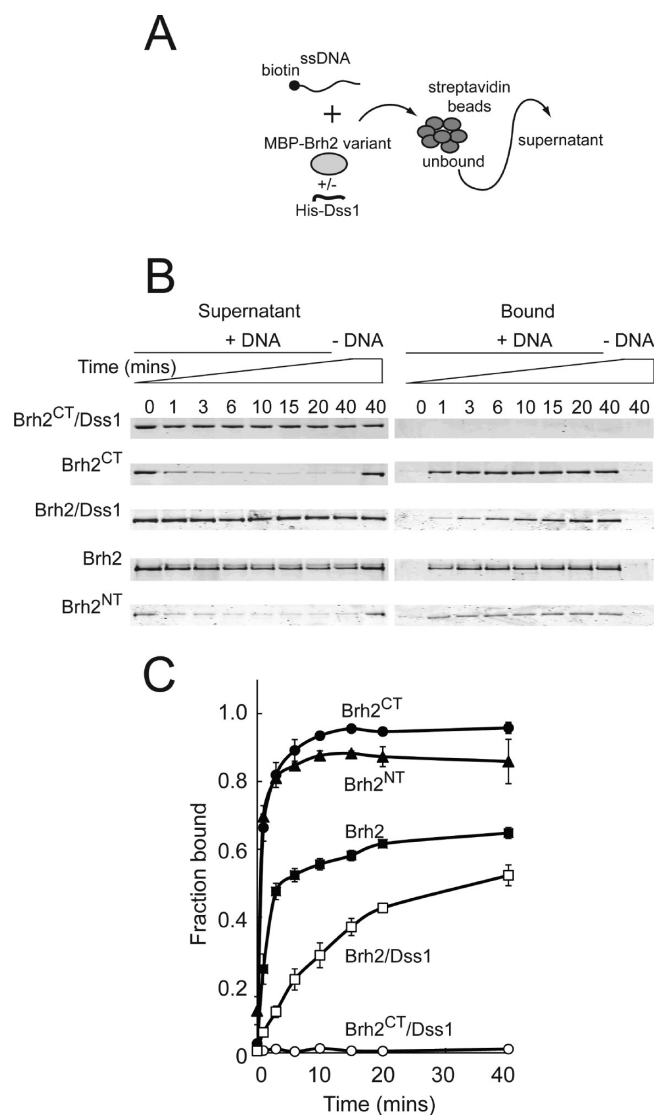


Figure 2. Dss1 and DNA binding activity of Brh2 truncations. (A) Schematic illustration depicting the protocol performed. (B) Reaction mixtures containing 150 nM Brh2 derivatives with or without Dss1 as illustrated and 66 nM 3'-biotinylated 60-mer. At the indicated times, streptavidin-coated paramagnetic particles were added to aliquots (30 μ L) of reaction mixtures to capture DNA and associated protein and then collected and analyzed by SDS gel electrophoresis. Representative gels are shown. (C) Quantification of the data. Error bars indicate standard deviations ($n = 2$).

DNA Binding Activity of Brh2 Truncated Forms and Dss1 Status. The dependence on Dss1 of Brh2 and derivatives harboring a Dss1-interacting CTD region led us to consider various possible underlying molecular mechanisms. We considered the possibility that the CTD might function analogously as a degron to target any protein attached to it for destruction unless stabilized by association with Dss1. However, we ruled this idea out because we had previously noted that steady-state levels of Brh2 did not appear to be affected in the absence of Dss1.¹³ Furthermore, using fluorescence microscopy to measure subnuclear focus formation of GFP-tagged proteins in live cells, we previously observed that the level of DNA damage-induced Brh2 foci was undiminished in the *dss1* mutant.¹¹ These results suggested that the critical function of Dss1 is not as a stabilizer of Brh2.

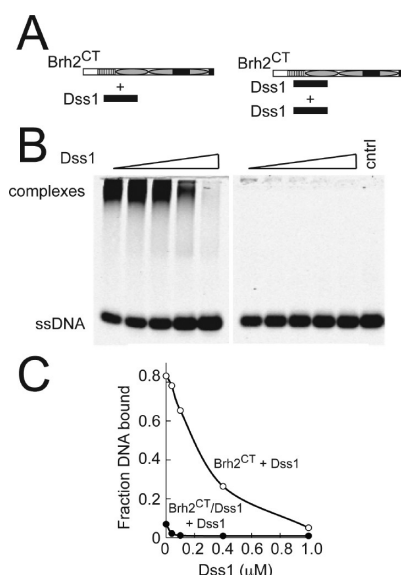


Figure 3. Dss1 inhibits DNA binding of Brh2^{CT}. (A) Schematic illustration of the MBP-Brh2–His-Dss1 derivatives employed (MBP and Dss1 domains not shown). (B) Reaction mixtures contained 3.3 nM IRD800 60-mer, 100 nM protein, and His-Dss1 at the indicated concentrations. After 15 min at 32 °C, samples were fixed with glutaraldehyde and analyzed by electrophoresis on 1% agarose gels. (C) Quantification of the data.

Another possibility we considered was that Dss1 controls the ability of Brh2 to associate with Rad51. However, we found no experimental evidence in support of this mechanism.¹¹ As an alternative, we considered the possibility that Dss1 influences the association of Brh2 with DNA and obtained some preliminary evidence for this notion showing that Dss1 and DNA appeared to counterbalance each other's interaction with Brh2.¹⁵

To examine the influence of Dss1 on the DNA binding activity of Brh2 in more detail, we used a streptavidin bead assay to monitor formation of Brh2 protein complexes bound to biotinylated ssDNA (Figure 2A). This assay has an advantage over electrophoretic mobility shift assays in that by capturing and removing beads from solution protein–DNA complexes, it offers a simple means for following rates of DNA binding. The DNA substrate was a biotinylated single-stranded oligonucleotide. Brh2 was tagged with maltose binding protein (MBP) and Dss1 with a hexahistidine leader sequence to aid selectivity and identification. After the MBP-Brh2–His-Dss1 heterodimer had been mixed with the labeled ssDNA, we monitored the physical association of MBP-Brh2 and His-Dss1 with ssDNA by capturing protein–DNA complexes on streptavidin-coated magnetic particles. For the sake of simplicity in the following discussion, MBP-Brh2 and derivatives as well as His-Dss1 will be mentioned without the MBP or His tag acronym.

Using this bead-based assay, we found that DNA binding activity was markedly influenced by Dss1 when a truncation of Brh2 retaining the cognate Dss1 interaction region was used (Figure 2B,C). Formation of protein–DNA complexes was rapid and efficient when the Brh2^{NT} fragment, which exhibits no physical interaction with Dss1 or inhibition by it,¹⁵ was assayed. Brh2^{CT} free of Dss1 was comparable in kinetics and efficiency. In contrast, the Brh2^{CT}–Dss1 heterodimer was not competent for DNA interaction. The full-length Brh2–Dss1

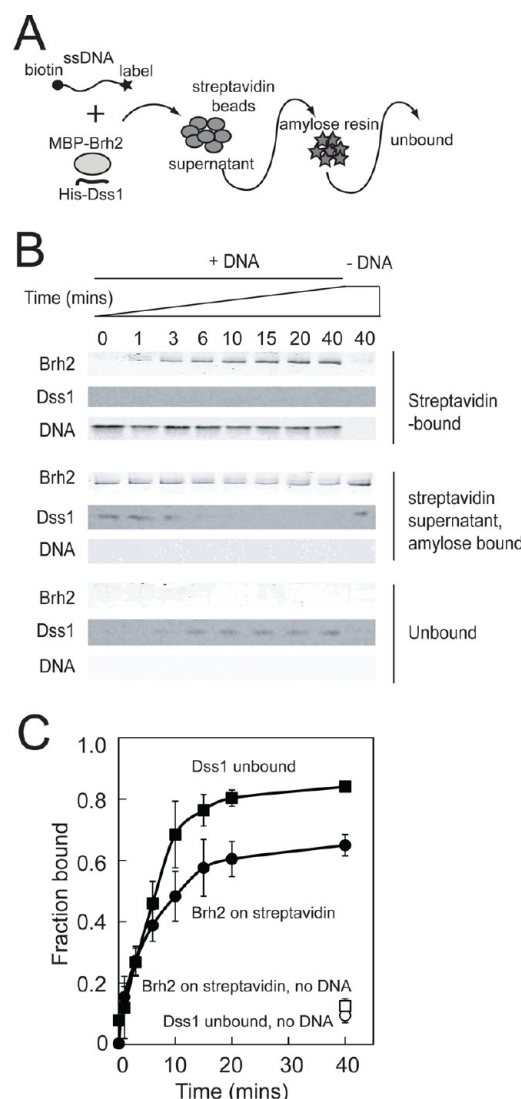


Figure 4. Brh2 and Dss1 dynamics during DNA binding. (A) Schematic illustration depicting the protocol performed. (B) Reaction mixtures contained 150 nM MBP-Brh2–His-Dss1 complex and 66 nM 3'-biotinylated 60-mer labeled with IRD800. At the indicated times, streptavidin-coated paramagnetic particles were added to aliquots (30 μL) of reaction mixtures to capture DNA and associated protein and then collected. Amylose resin was added to the supernatant to capture MBP-Brh2 complexes. SDS sample buffer was added to the streptavidin-bound, amylose-bound, and unbound fractions, and these were analyzed by SDS gel electrophoresis. Components were visualized as described in Experimental Procedures. Representative gels and blots are shown. (C) Quantification of the data. Error bars indicate standard deviations ($n = 2$).

heterodimer appeared to respond in an intermediate fashion. It was slow in binding DNA by comparison with the Brh2-free form, but complexes ultimately formed at a level nearing the extent of the Brh2-free form. The basis for the lower rate and extent of reaction of full-length Brh2 compared to those of Brh2^{NT} and Brh2^{CT} is not known, but it might stem from impaired association of the biotinylated oligonucleotide–protein complex with streptavidin-coated magnetic particles due to the larger bulk of the protein. These findings support the notion that interaction of Dss1 with the CTD domain of Brh2 is an important dynamic that constrains its association with DNA.

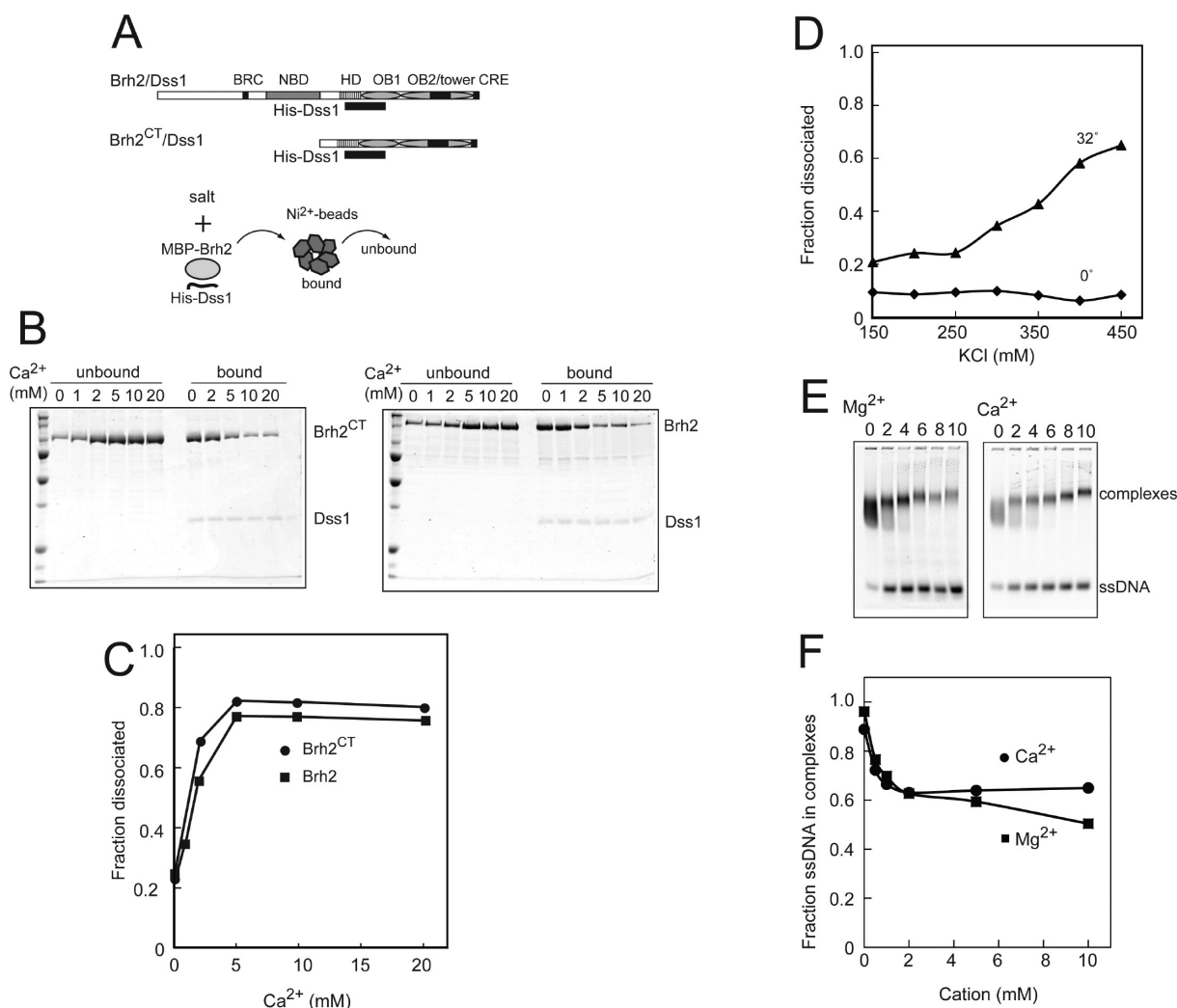


Figure 5. Salt-dependent dissociation of Brh2–Dss1 complexes. (A) Schematic illustration of the MBP–Brh2–His–Dss1 derivatives employed (MBP and Dss1 domains not shown) and the protocol performed. (B) Reaction mixtures (50 μ L) contained 460 nM Brh2 or derivative prepared as a complex with His–Dss1. After 15 min at 32 $^{\circ}$ C, Ni²⁺–NTA agarose was added to capture His–Dss1 and associated Brh2. Samples were analyzed by SDS gel electrophoresis. (C) Quantification of the data in panel B. (D) Reactions were performed as described above with the indicated concentrations of KCl at 0 or 32 $^{\circ}$ C, and results are presented after quantification. (E) Reaction mixtures contained 3.3 nM IRD800 80-mer, 100 nM protein, and the indicated concentrations (millimolar) of Mg²⁺ or Ca²⁺. After 40 min at 32 $^{\circ}$ C, glutaraldehyde was added to stabilize the protein–DNA complexes and samples were electrophoresed on 1% agarose gels. (F) Quantification of the data in panel E.

Excess Dss1 Inhibits DNA Binding. As was shown in structural studies with the mammalian BRCA2 DBD–DSS1 heterodimer,⁷ it was found that Brh2 forms a tight complex with Dss1^{11,12} after being co-expressed in insect or bacterial cells. We expected, therefore, that in a purified in vitro system Dss1 would reassociate with the Brh2 CTD according to Le Chatelier’s principle. If so, then according to our observations described above, it would be predicted that DNA binding should be severely quenched. To test this notion, we added increasing amounts of Dss1 to Brh2^{CT} and measured the DNA binding activity by a standard gel mobility shift assay (Figure 3). It was evident that adding back Dss1 resulted in strong attenuation of DNA binding activity, it dropping to the level of activity exhibited by the Brh2^{CT}–Dss1 heterotypic complex. These findings suggest that Brh2 exists in a dynamic equilibrium with Dss1 and support the notion that Dss1 status is a factor influencing the DNA binding potential of Brh2.

Dissociation of Dss1 from Brh2 during the Course of DNA Binding. We tracked the dynamics of Brh2 and Dss1

during DNA binding using a pull-down methodology as this procedure offered a means of tracking the disposition of all components in the reaction mixture (Figure 4A). The DNA substrate was a biotinylated single-stranded oligonucleotide labeled with the fluorescent dye IRD800. As described above, Brh2 was tagged with maltose binding protein (MBP) and Dss1 with a hexahistidine leader sequence to aid selectivity and identification. We monitored association of MBP–Brh2 and His–Dss1 with ssDNA by capturing protein–DNA complexes on streptavidin beads. To analyze the status of MBP–Brh2 not bound to ssDNA for associated His–Dss1, free MBP–Brh2 was captured on amylose resin. ssDNA, MBP–Brh2, and His–Dss1 were then assayed after both the streptavidin beads and amylose resin had been stripped with detergent, and then components were analyzed after gel electrophoresis. The ssDNA oligonucleotide was visualized by fluorescence; MBP–Brh2 was detected by protein staining, and His–Dss1 was detected using a His tag specific antibody.

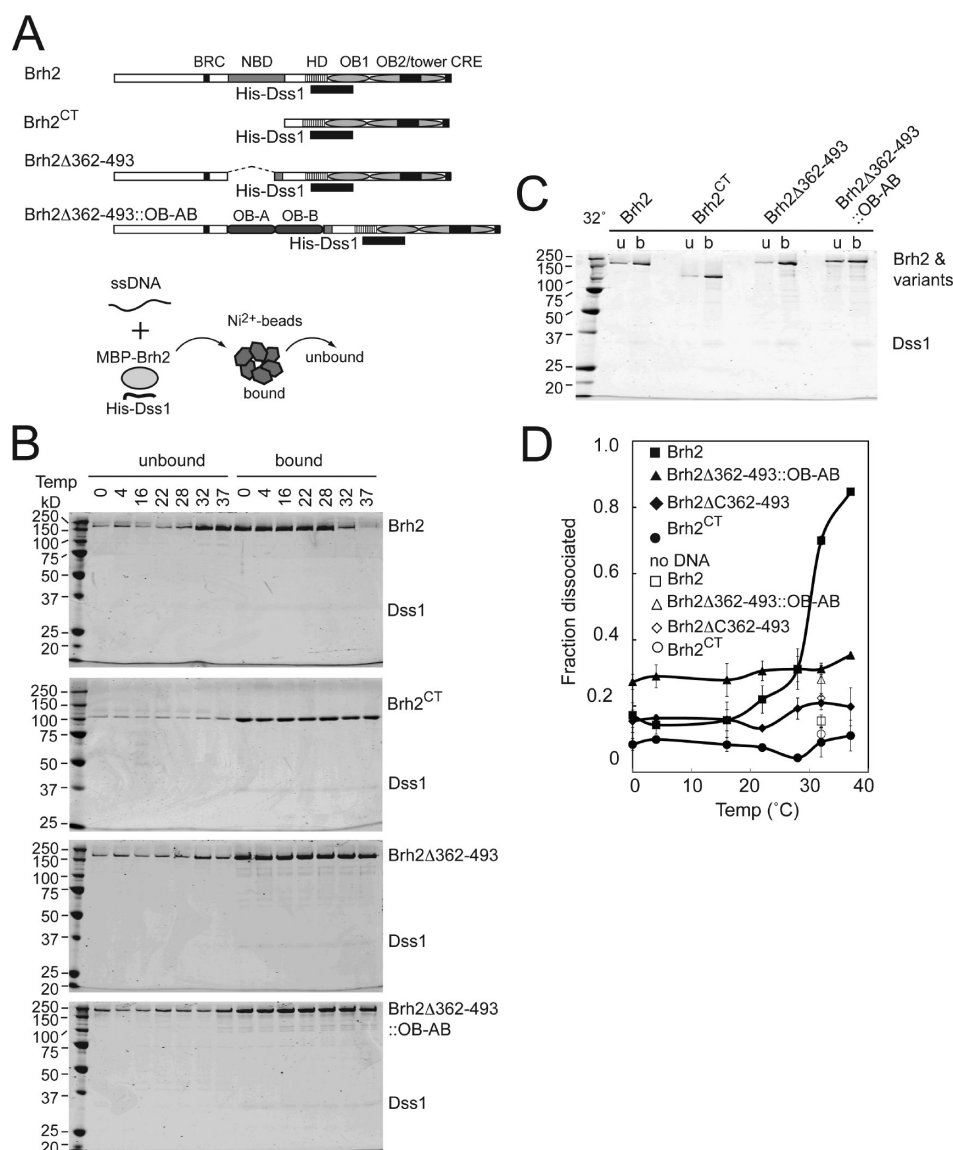


Figure 6. DNA-promoted dissociation of Brh2–Dss1 complexes. (A) Schematic illustration of the MBP–Brh2–His–Dss1 derivatives employed (MBP and Dss1 domains not shown) and the protocol performed. (B) Reaction mixtures (50 μ L) contained 160 nM 60-mer and 460 nM Brh2 or derivative prepared as a complex with His–Dss1. After 15 min at the indicated temperature, samples were analyzed by SDS gel electrophoresis. (C) Reaction mixtures were performed as described above at 32 $^{\circ}$ C but in the absence of the 60-mer oligonucleotide. Samples unbound (u) samples bound (b). (D) Quantification of the data. Error bars indicate standard deviations ($n = 2$).

Over the course of ~ 20 min, we observed a slow rise and then a plateau in the amount of Brh2 bound to ssDNA on the streptavidin beads (Figure 4B,C). In parallel was a concomitant release of Dss1 in a form unassociated with Brh2, free in solution. These observations reinforce the notion that Brh2 appears to associate with either DNA or Dss1, but not with both simultaneously, and suggest that ssDNA promotes dissociation of the Brh2–Dss1 heterodimer.

Cation-Promoted Dissociation of Dss1 from Brh2. In a survey of conditions promoting dissociation of the Brh2–Dss1 complex, we noticed that in solutions containing either monovalent or divalent cations there was an elevated level of dissociation of Dss1 over time. To quantify this behavior, we used Ni²⁺-NTA agarose beads to capture His–Dss1 and determined the level of associated native Brh2 or Brh2^{CT} derivative bound to the beads and in the unbound fraction (Figure 5A). The effect of Ca²⁺ is depicted as a representative example of divalent cation (Figure 5B,C). Similarly, the effect of

K⁺ as a representative monovalent cation is shown (Figure 5D). As is evident, a considerably higher concentration of K⁺ is required to achieve a level of dissociation comparable to that reached with Ca²⁺ at 32 $^{\circ}$ C. It is also evident that dissociation of Dss1 from Brh2 is attenuated at lower temperatures. The DNA binding activity of the Brh2–Dss1 complex is partially diminished in the presence of up to 2 mM divalent cation but then remains fairly constant up to 10 mM (Figure 5E,F). This suggests that DNA binding by the Dss1-free form of Brh2 is tolerant of moderate divalent cation concentrations. These results illustrate that the Brh2 CTD–Dss1 complex responds to environmental conditions such as ionic strength and that the stability is the same regardless of the CTD context, i.e., as an isolated domain or as part of the native protein. The findings support the idea that the Brh2–Dss1 complex in solution is in a dynamic equilibrium.

Domain Dependence in the Release of Dss1 from Brh2. When DNA was present, there was a striking effect of

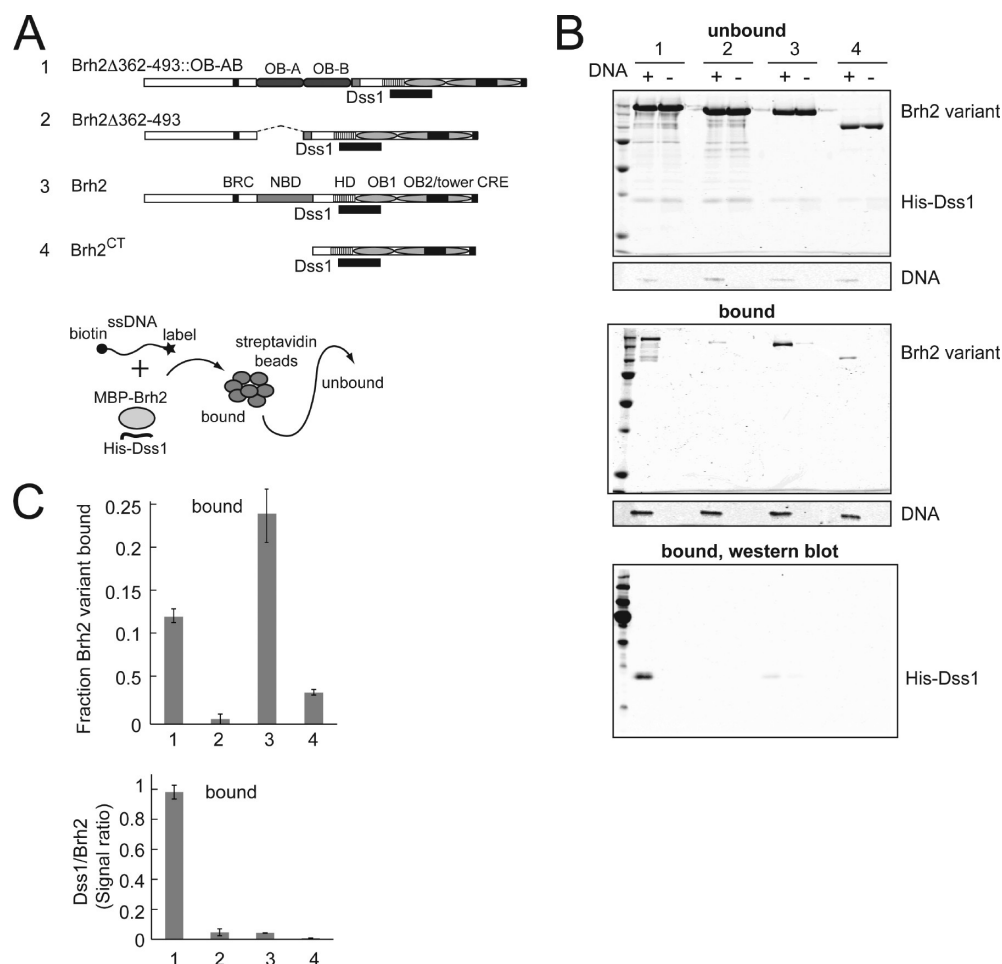


Figure 7. Dynamics of association of Dss1 with Brh2 derivatives. (A) Schematic illustration of the MBP-Brh2–His-Dss1 derivatives employed (MBP and Dss1 domains not shown) and the protocol performed. (B) Reaction mixtures (50 μ L) contained 860 nM Brh2–Dss1 derivative and 133 nM biotinylated labeled 60-mer as shown. After 20 min at 32 $^{\circ}$ C, streptavidin-coated paramagnetic particles were added and the bound and unbound fractions were analyzed by SDS gel electrophoresis. (C) Quantification of the data. Error bars represent standard deviations ($n = 2$).

temperature on the stability of the Brh2–Dss1 complex. Above 28 $^{\circ}$ C, dissociation became markedly pronounced over a 40 min time period. The enhanced dissociation was dependent upon an intact N-terminal domain. In contrast, complexes of Dss1 and Brh2 derivatives that lacked the N-terminal domain or contained a heterologous DNA-binding domain (Figure 6A) were all unresponsive to temperature compared to the natural Brh2–Dss1 heterodimer (Figure 6B,C). Because DNA binds avidly to the NBD but is unaffected by Dss1, these observations imply that ejection of Dss1 from the CTD is linked mechanistically to association of DNA with the NBD.

To verify these findings, we used an alternative pull-down procedure to analyze the composition of complexes formed upon binding to biotinylated ssDNA. Protein–DNA complexes captured with streptavidin beads were examined after heat denaturation and gel electrophoresis (Figure 7A). Of the different Brh2 forms tested, native Brh2 was captured in the highest abundance, followed by the Brh2 derivative with RPA70 OB-AB in place of NBD. In the latter, there was substantial Dss1 that remained associated with the bound fraction, while in the complexes with native Brh2, the level of Dss1 was at least 20-fold lower (Figure 7B,C). The Brh2 derivatives without the N-terminal domain or the NBD were captured inefficiently because of the reduced affinity for DNA. The low level of protein captured had little associated Dss1, suggesting that

these complexes represented the class that had already spontaneously lost Dss1. These findings reinforce the observations described above that the release of Dss1 is concomitant with binding of Brh2 to DNA, and that the release is contingent upon the presence of the natural NBD.

Temperature-Dependent DNA Binding. Given the above observations that Brh2 and derivatives lacking Dss1 bind DNA more avidly than when complexed with Dss1 and that elevated temperature accelerates dissociation of the Brh2–Dss1 complex, we reasoned that DNA binding activity would likely be enhanced with an increasing temperature. By a mobility shift assay, it was apparent that the native Brh2–Dss1 complex became more avid in DNA binding when the temperature passed a threshold of \sim 28 $^{\circ}$ C mirroring the temperature dependence noted for the dissociation of the Brh2–Dss1 complex (Figure 8). Presumably, the binding activity at the lower temperatures represents the action of the NBD, while the elevated activity at higher temperatures reflects the added contribution of the Dss1-free CTD. Brh2 free of Dss1 showed no temperature dependence in DNA binding presumably because its DNA binding potential was already fully activated. The Brh2^{CT} variant exhibited an only slight stimulation for DNA binding above the threshold temperature. Presumably, this stimulation reflects the strong DNA binding activity of a low level of Dss1-free Brh2^{CT} that is present.

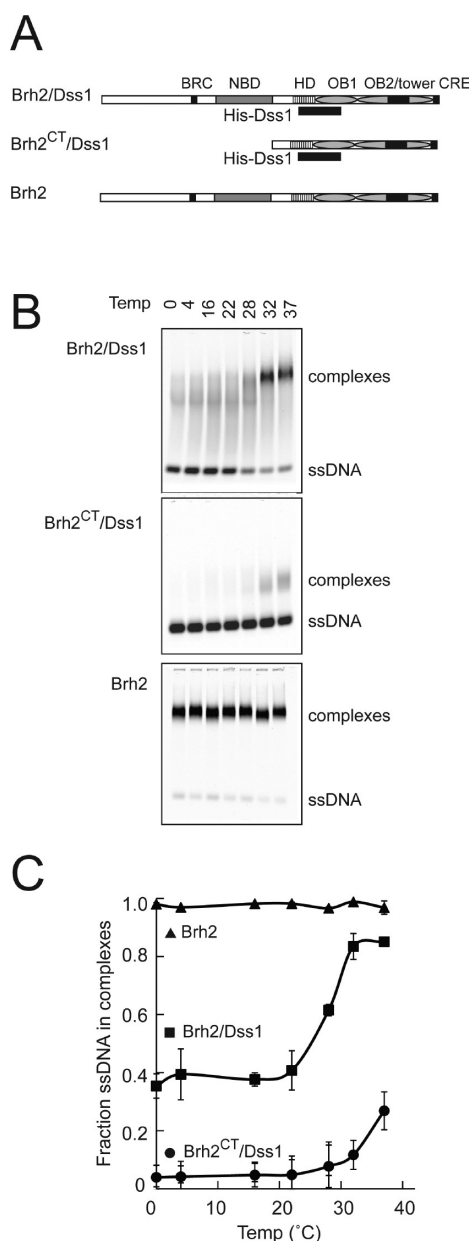


Figure 8. Temperature-dependent DNA binding. (A) Schematic illustration of the MBP-Brh2–His-Dss1 derivatives employed (MBP domains not shown). (B) DNA binding reaction mixtures contained 3.3 nM IRD800 80-mer and 100 nM protein. After 40 min at the indicated temperature, samples were placed on ice and glutaraldehyde was added to stabilize the protein–DNA complexes. After 10 min, samples were electrophoresed on 1% agarose gels. Representative gels are shown. (C) Quantification of the data. Error bars represent standard deviations ($n = 2$).

DISCUSSION

Three conclusions can be drawn from the findings presented here. First, Dss1 is capable of exerting control over Brh2 and various derivatives containing heterologous DNA-binding domains only when there is a cognate Dss1-interacting surface present. Second, Dss1 attenuates the DNA binding potential of Brh2. Third, the N-terminal domain of Brh2 mediates ejection of Dss1 in the presence of DNA above a certain threshold temperature. The findings suggest that Dss1 serves as a component of a molecular switching process to regulate the participation of Brh2 in DNA repair.

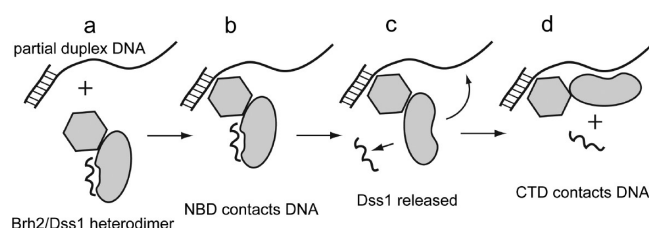


Figure 9. Dss1 regulates DNA binding by Brh2. Hypothetical model for binding of Brh2 to DNA. (a) Brh2 illustrated as an N-terminal domain (hexagon) containing the NBD and CTD (deformed oval) in complex with Dss1 (squiggle) approaches partially duplex DNA with a protruding tail. (b and c) As the N-terminal domain contacts DNA, there is an induced allosteric change resulting in the release of Dss1 and the concomitant opening of the DNA binding surface of the CTD indicated by the change to a sausage shape. (d) The Brh2–DNA complex is free of Dss1 and stabilized through two appropriately positioned DNA binding regions.

Dss1 appears to function in activating native Brh2. In the absence of Dss1, cells are as sensitive to radiation as mutants without Brh2 or Rad51.⁹ From imaging studies using fluorescence microscopy to visualize and track labeled proteins, it has been observed that following radiation damage to cells Rad51 reorganizes into discrete subnuclear foci, sites presumably representing factories for DNA repair.¹³ While Rad51 focus formation depends on Brh2 and Dss1, Brh2 focus formation still occurs in the absence of Dss1,¹¹ suggesting Brh2 is still recruited to sites of damage but is incapable of acting without Dss1. Together with the finding that Dss1 forms a tight complex with Brh2, these observations imply that Dss1 acts as an activator of Brh2.

Brh2 is highly plastic in being able to tolerate large truncations or deletions. Derivatives in which either the N-terminal or C-terminal DNA-binding domain has been removed or replaced with a heterologous DNA-binding domain can still maintain proficiency in DNA repair and recombination.^{16,19} Brh2 derivatives without the C-terminal domain, including the Dss1 interaction region, which are active by virtue of an added heterologous DNA-binding domain, are independent of Dss1. On the other hand, active Brh2 derivatives without the N-terminal DNA-binding domain or with a replacement heterologous DNA-binding domain but with the cognate Dss1-interacting surface are dependent on Dss1. Thus, it appears that Brh2 and derivatives become subjugated under Dss1 control whenever a cognate Dss1-interacting surface is present. What purpose could be served by such an arrangement?

The likely answer seems to be that the system was developed as a fine-tuning regulatory mechanism for controlled release of the full DNA binding potential of Brh2. Dss1 associated with Brh2's CTD restrains interaction of the native protein with DNA, such that initial contact appears to be mediated through the alternate DNA-binding domain in the N-terminal region. This restraint is particularly evident with the Brh2^{CT} derivative, which exhibits poor DNA binding when complexed with Dss1 but strong DNA binding when free of Dss1. As Dss1 dissociates from native Brh2, DNA binding is potentiated. Release of Dss1 allows the deployment of the DNA binding activity associated with the CTD, which unleashes the full DNA binding potential of the native protein. Thus, Dss1 dictates order in how Brh2 domains associate with DNA.

Upon addition of DNA, the N-terminal part of Brh2 appears to communicate in some way with the C-terminal part to allow Dss1 release. This communication requires the native configuration of the NBD and CTD and is enhanced by temperature above a threshold of $\sim 28^\circ\text{C}$. Starting with the Brh2–Dss1 heterodimer in the native state, we observed that protein–DNA complexes recovered after DNA binding contained little Dss1. However, by comparison, the Brh2 derivative having the heterologous OB–AB module in place of NBD, DNA-bound complexes contained abundant Dss1. Therefore, it appears that release of Dss1 from the CTD is promoted specifically by the NBD. The pronounced effect of temperature on Dss1 release with DNA addition is striking, but the basis of the effect is unknown. It might indicate the formation of a metastable tripartite Brh2–Dss1–DNA complex that relaxes to a stable binary Brh2–DNA complex when the thermal energy surpasses a certain threshold.

In light of all of the observations presented here, we suggest a model (Figure 9) in which there is an allosteric change in Brh2 protein conformation resulting from association of DNA with the NBD with the consequence that Dss1 dissociates, thereby freeing for deployment the DNA binding potential inherent in the CTD OB-containing module. Accordingly, Dss1 appears to function as a servomechanism imposing a constraint on Brh2 and dictating order in the manner its individual domains contact DNA. The model is provocative and raises interesting questions about the biological significance of a sequential and ordered actualization of Brh2's DNA binding capacity. Such a mechanism could provide a means for a temporal and directed progression in the DNA binding process. While it is clear that truncated forms of Brh2 with only a single DNA-binding domain are active in some aspects of DNA repair, resolution of stalled-replication-associated DNA lesions requires both DNA-binding domains.¹⁹ The dual DNA binding modality with hierarchical progression might help intricately position Brh2 for precise, appropriate, and effective delivery of Rad51 to DNA lesions and allow accurate and well-controlled DNA repair and restart of stalled or broken replication forks. In any case, the model deserves further exploration. Only additional research will illuminate the precise mechanism of the Brh2–Dss1 interplay and reveal a more definitive answer to the question of why pivotal cellular functions of Brh2 are dependent on a small protein such as Dss1.

AUTHOR INFORMATION

Corresponding Author

*Telephone: (212) 746-6510. Fax: (212) 746-8587. E-mail: wkhollo@med.cornell.edu.

Funding

This work was supported in part by Grants GM42482 and GM79859 from the National Institutes of Health.

Notes

The authors declare no competing financial interest.

ACKNOWLEDGMENTS

We thank Dr. Jeanette Sutherland of this laboratory for discussion and comments on the manuscript.

ABBREVIATIONS

BRC, BRCA2-associated Rad51-binding motif; CT, carboxy-terminal; CTD, C-terminal domain; DBD, DSS1/DNA-binding domain; ds, double-stranded; HEPES, *N*-(2-hydroxyethyl)-

piperazine-*N'*-(2-ethanesulfonic acid); IRD, infrared dye; six-His tag, hexahistidine tag; MBP, maltose binding protein; NT, amino-terminal; NTA, nitrilotriacetate agarose; OB, oligonucleotide/oligosaccharide binding; ss, single-stranded; UV, ultraviolet.

REFERENCES

- (1) Heyer, W. D., Ehmsen, K. T., and Liu, J. (2010) Regulation of homologous recombination in eukaryotes. *Annu. Rev. Genet.* 44, 113–139.
- (2) Holthausen, J. T., Wyman, C., and Kanaar, R. (2010) Regulation of DNA strand exchange in homologous recombination. *DNA Repair* 9, 1264–1272.
- (3) San Filippo, J., Sung, P., and Klein, H. (2008) Mechanism of eukaryotic homologous recombination. *Annu. Rev. Biochem.* 77, 229–257.
- (4) Holloman, W. K. (2011) Unraveling the mechanism of BRCA2 in homologous recombination. *Nat. Struct. Mol. Biol.* 18, 748–754.
- (5) Pellegrini, L., Yu, D. S., Lo, T., Anand, S., Lee, M., Blundell, T. L., and Venkitaraman, A. R. (2002) Insights into DNA recombination from the structure of a RAD51–BRCA2 complex. *Nature* 420, 287–293.
- (6) Rajendra, E., and Venkitaraman, A. R. (2010) Two modules in the BRC repeats of BRCA2 mediate structural and functional interactions with the RAD51 recombinase. *Nucleic Acids Res.* 38, 82–96.
- (7) Yang, H., Jeffrey, P. D., Miller, J., Kinnucan, E., Sun, Y., Thoma, N. H., Zheng, N., Chen, P. L., Lee, W. H., and Pavletich, N. P. (2002) BRCA2 function in DNA binding and recombination from a BRCA2–DSS1–ssDNA structure. *Science* 297, 1837–1848.
- (8) Lo, T., Pellegrini, L., Venkitaraman, A. R., and Blundell, T. L. (2003) Sequence fingerprints in BRCA2 and RAD51: Implications for DNA repair and cancer. *DNA Repair* 2, 1015–1028.
- (9) Kojic, M., Yang, H., Kostrub, C. F., Pavletich, N. P., and Holloman, W. K. (2003) The BRCA2-interacting protein DSS1 is vital for DNA repair, recombination, and genome stability in *Ustilago maydis*. *Mol. Cell* 12, 1043–1049.
- (10) Kojic, M., Kostrub, C. F., Buchman, A. R., and Holloman, W. K. (2002) BRCA2 homolog required for proficiency in DNA repair, recombination, and genome stability in *Ustilago maydis*. *Mol. Cell* 10, 683–691.
- (11) Zhou, Q., Kojic, M., Cao, Z., Lisby, M., Mazloun, N. A., and Holloman, W. K. (2007) Dss1 interaction with Brh2 as a regulatory mechanism for recombinational repair. *Mol. Cell. Biol.* 27, 2512–2526.
- (12) Yang, H., Li, Q., Fan, J., Holloman, W. K., and Pavletich, N. P. (2005) The BRCA2 homologue Brh2 nucleates RAD51 filament formation at a dsDNA–ssDNA junction. *Nature* 433, 653–657.
- (13) Kojic, M., Zhou, Q., Lisby, M., and Holloman, W. K. (2005) Brh2–Dss1 interplay enables properly controlled recombination in *Ustilago maydis*. *Mol. Cell. Biol.* 25, 2547–2557.
- (14) Zhou, Q., Kojic, M., and Holloman, W. K. (2009) DNA-binding Domain within the Brh2 N Terminus Is the Primary Interaction Site for Association with DNA. *J. Biol. Chem.* 284, 8265–8273.
- (15) Zhou, Q., Mazloun, N., Mao, N., Kojic, M., and Holloman, W. K. (2009) Dss1 regulates interaction of Brh2 with DNA. *Biochemistry* 48, 11929–11938.
- (16) Kojic, M., Zhou, Q., Fan, J., and Holloman, W. K. (2011) Mutational analysis of Brh2 reveals requirements for compensating mediator functions. *Mol. Microbiol.* 79, 180–191.
- (17) Kojic, M., Zhou, Q., Lisby, M., and Holloman, W. K. (2006) Rec2 interplay with both Brh2 and Rad51 balances recombinational repair in *Ustilago maydis*. *Mol. Cell. Biol.* 26, 678–688.
- (18) Mazloun, N., Zhou, Q., and Holloman, W. K. (2007) DNA binding, annealing, and strand exchange activities of Brh2 protein from *Ustilago maydis*. *Biochemistry* 46, 7163–7173.
- (19) Kojic, M., and Holloman, W. K. (2012) Brh2 domain function distinguished by differential cellular responses to DNA damage and replication stress. *Mol. Microbiol.* 83, 351–361.

(20) Lange, A., Mills, R. E., Lange, C. J., Stewart, M., Devine, S. E., and Corbett, A. H. (2007) Classical nuclear localization signals: Definition, function, and interaction with importin α . *J. Biol. Chem.* 282, 5101–5105.